

Dwarf Nova Oscillations and Quasi-Periodic Oscillations in Cataclysmic Variables, IV. Observations of Frequency Doubling and Tripling in VW Hyi.

Brian Warner[★] and Patrick A. Woudt[†]

Department of Astronomy, University of Cape Town, Private Bag, Rondebosch 7700, South Africa

2005 March 25

ABSTRACT

We present new observations of the rapid oscillations in the dwarf nova VW Hyi, made late in outburst. These dwarf nova oscillations (DNOs) increase in period until they reach 33 s, when a transition to a strong 1st harmonic and weak fundamental takes place. After further period increase the 2nd harmonic appears; often all three components are present simultaneously. This 1:2:3 frequency suite is similar to what has been seen in some neutron star and black hole X-Ray binaries, but has not previously been seen in a cataclysmic variable. When studied in detail the fundamental and 2nd harmonic vary similarly in phase, but the 1st harmonic behaves independently, though keeping close to twice the frequency of the fundamental. The fundamental period of the DNOs, as directly observed or inferred from the harmonics, increases to ~ 100 s before the oscillation disappears as the star reaches quiescence. Its maximum period is close to that of the ‘longer period’ DNOs observed in VW Hyi. The quasi-periodic oscillations (QPOs), which have fundamental periods 400 – 1000 s, behave in the same way, showing 1st and 2nd harmonics at approximately the same times as the DNOs. We explore some possible models. One in which the existence of the 1st harmonic is due to transition from viewing a single accretion region to viewing two regions, and the rate of accretion onto the primary is modulated at the frequency of the 1st harmonic, as in the ‘beat frequency model’, can generate the suite of DNO frequencies observed. But the behaviour of the QPOs is not yet understood.

Key words: accretion, accretion discs – binaries: close, dwarf novae, cataclysmic variables – stars: oscillations – stars: individual: VW Hyi, EK TrA – X-Rays: stars

1 INTRODUCTION

Many dwarf novae show rapid (typical periods 5 – 40 s) low amplitude brightness oscillations during outburst, and some nova-like variables show similar modulations. These have been actively studied since their discovery some thirty years ago (Warner & Robinson 1972) and are known collectively as dwarf nova oscillations (DNOs). They show a systematic period-luminosity relationship during outburst, with minimum period at maximum bolometric luminosity, and are of moderate coherence near maximum but usually appear to become increasingly incoherent near the return to quiescence. The DNO periods have been observed to range over a factor of more than two in some dwarf novae. The short periods indicate that the source of these modulations

is close to the white dwarf primary in these cataclysmic variables (CVs); this is confirmed by the appearance of oscillations of substantial amplitude in soft X-Ray and EUV flux during the outbursts of, e.g., the nearby dwarf novae VW Hyi and SS Cyg. Evidently the mass transfer from the accretion disc to the primary is strongly modulated at the DNO period.

The DNOs were reviewed in Warner (1995a); updates are given in Warner (1995b), in the first two papers in this series (Woudt & Warner 2002: hereafter Paper I; Warner & Woudt 2002: hereafter Paper II) and in Warner (2004). A model in which the accretion flow close to the primary is controlled by the magnetic field generated in a rapidly rotating equatorial belt, formed as a result of the high rate of accretion, has been proposed (Warner 1995b; Paper II); this is basically an intermediate polar structure, including a truncated accretion disc, but where only the belt receives the accreting angular momentum; the belt is magnetically coupled to the accretion disc but is able to slip relative to

[★] email: warner@physci.uct.ac.za

[†] email: pwoudt@circinus.ast.uct.ac.za

the body of the white dwarf primary. This Low Inertia Magnetic Accretor (LIMA) model (which was first proposed by Paczynski (1978)) allows large variations in DNO periods, and also explains the rapid deceleration of the DNOs observed in VW Hyi near the end of its outburst (Papers I and II) – from the effect of outward propelling of gas as the belt continues to revolve rapidly after the mass transfer rate (\dot{M}) diminishes. It is probable that the inner edge of the truncated disc is close to the corotation radius (where the Keplerian period in the disc equals the rotation period of the primary), even when propelling is present, as argued by Rappaport, Fregeau & Spruit (2004). Furthermore, the rotation period of the field carried round by the equatorial belt will rarely be exactly the same as the period of the inner edge of the disc – the belt is continually being spun up or down by its magnetic connection to the disc. This corresponds to the model with large Θ in the 3D simulations of accretion from a disc onto an inclined dipole by Romanova et al. (2004), which is the model in which they find rapid quasi-periodic luminosity variations. In these 3D models, unlike the simple 2D LIMA model, the field inflates, opens out and reconnects, but the process is still driven by differential rotation between star and disc (see Uzdensky (2004) for a review).

The optical DNOs are the result of soft X-Ray and EUV emission from the accretion zones creating a ‘beam’ that sweeps around and is reprocessed to longer wavelengths by the surface of the disc or anything else it illuminates. Another DNO component can come from the accretion zone itself.

Independent deduction of the existence of a spinning belt in VW Hyi and in other dwarf novae has been obtained from HST and FUSE spectroscopic observations. Spectra taken after outburst can only be modeled by composite spectra, in the case of VW Hyi comprising a white dwarf with projected rotational velocity $v \sin i$ in the range 300 – 400 km s⁻¹ and a hotter component of small area and $v \sin i$ 3000 – 4000 km s⁻¹ (Sion et al. 1996; Gänsicke & Beuermann 1996; Godon et al. 2004; Sion et al. 2004a,b,c). The spinning accretion belt lasts for at least 14 days after a superoutburst (Sion et al. 2004b).

There is a second kind of DNO with periods about 4 times those of the standard DNOs, with little or no dependence on accretion luminosity. These are termed longer period DNOs: lpDNOs (Warner, Woudt & Pretorius: hereafter Paper III; Pretorius 2004).

In addition to the two types of DNO, there are large amplitude modulations with periods about 15 times larger than those of the DNOs, and much shorter coherence, known as quasi-periodic oscillations (QPOs). In Paper II we proposed that these are caused by traveling waves excited in the inner disc – reprocessing and obscuring radiation from the bright central regions of the disc. Furthermore, the occasional appearance of ‘double DNOs’ with frequency difference equal to the QPO frequency are attributed to the DNO ‘beam’ sweeping around and being partly reprocessed by the progradely traveling vertically thickened disc. We should therefore in general be prepared to distinguish between ‘direct’ DNOs, which arise from reprocessing from the disc, and what we will call here ‘synodic’ DNOs, which are reprocessed from some moving site (this is discussed in more detail in Section 3). Whereas the direct DNOs are observed

to be sinusoidal, the synodic DNOs commonly possess significant amplitude at their first harmonic. Because the synodic DNOs are observed to be reprocessed from a progradely moving source we do not consider a magnetically warped and precessing inner disc, which moves retrogradely (Pfeiffer & Lai 2004).

In VW Hyi we observed evolution of both the DNO and the QPO periods but the ratio $R = P_{QPO}/P_{DNO}$ remained almost constant at ~ 15 (Paper I). It was pointed out that a similar ratio is seen in the high and low frequency QPOs observed in X-Ray binaries (Beloni, Psaltis & van der Klis 2002), and that in fact (identifying DNOs and QPOs in CVs as the equivalent of the two kinds of QPOs in X-Ray binaries) the behaviour of VW Hyi forms an extension two orders of magnitude lower in frequency of the two-QPO correlation seen in the latter. An extension to even lower frequencies in other CVs has since been observed (Mauche 2002; Paper III).

The importance of further observations of DNOs and QPOs in CVs, where they are more easily analysed than in the X-Ray binaries, is evident. The rich set of phenomena exhibited by VW Hyi (Papers I and II) makes this a prime target for further study. In Section 2 we report further high speed photometric measurements of VW Hyi made towards the end of outburst, supplementing those already presented in Paper I, and revealing the occurrence of harmonic 1:2:3 ratios of periods late in outburst. In Section 3 we consider possible interpretations in terms of magnetically controlled accretion; in Section 4 we compare our VW Hyi results with those seen in X-Ray binaries and in Section 5 we briefly summarize the current state of play.

2 PHOTOMETRIC OBSERVATIONS OF VW HYI

The VW Hyi data presented here are a combination of some archival data (Paper I) and a large number of new observations. The latter have been made selectively towards the ends of outbursts, with the specific aim of studying the DNO and QPO behaviours just as the star returns to quiescence. It is in this phase of outburst that apparent frequency doubling has been observed, but the evolution from fundamental to first harmonic seemed unstructured, even chaotic, and could not be followed with the limited observational material available (Paper I). All new observations were made with the UCT CCD Photometer (O’Donoghue 1995) operating in frame-transfer mode (resulting in zero dead-time and therefore maximum time-resolution) on the 74-in or 40-in reflectors at the Sutherland site of the South African Astronomical Observatory. Fortunately VW Hyi is circumpolar at Sutherland, which provides an extended observing season.

In Table 1 we give the log of the high speed photometric runs on VW Hyi that are analysed in this paper. These include a few of the runs already studied in Paper I. Integration times (Column 4 in Table 1) range between 2 and 6 seconds. In general, observations were taken in white light (no filter, see Column 3 in Table 1). On a few occasions, a filter was used to avoid saturating the UCT CCD when observing with the 74-in telescope. The UCT CCD data are subjected to a standard data reduction routine (including flat fielding using sky flat fields) which outputs aper-

Table 1. An overview of a section of our data archive of VW Hyi. Observations in the late stages of decline from outburst with DNOs present.

Run	Tel.	Filter	HJD Start +244 0000	t_{in} (sec)	Outburst Type [†]	$T = 0^*$ (days)	Length (hours)	Range T (days)	DNOs**	QPO
S0018	20-in	–	1572.49752	2	Normal (L)	1572.75	2.04	−0.25 → −0.17	F	–
S6133	74-in	I	11785.54592	2	Normal (L)	11785.75	2.84	−0.20 → −0.09	F	–
S6184	40-in	–	11957.27611	5	Normal (L)	11957.25	1.68	0.03 → 0.10	F	✓
S6059	40-in	–	11580.27697	4	Normal (M)	11580.20	5.27	0.08 → 0.30	F	✓
S0127	40-in	–	1677.29328	4	Super	1677.20	3.77	0.09 → 0.25	F	✓
S7961	40-in	–	13463.22526	6	Normal (L)	13463.10	4.03	0.13 → 0.34	F 1	–
S2915	40-in	–	4937.28242	4	Normal (L)	4937.10	0.73	0.18 → 0.21	1	–
S1307	40-in	–	2354.38968	4	Normal (M)	2354.20	1.33	0.19 → 0.25	1	✓
S7311	74-in	B	13139.19081	4	Normal (M)	13138.95	5.41	0.24 → 0.47	1 2	✓
S7342	40-in	–	13155.19077	5	Normal (M)	13154.90	3.07	0.29 → 0.42	F 1 2	✓
S6316	40-in	–	12354.23650	5	Normal (L)	12353.95	5.72	0.29 → 0.53	1	✓
S6138	40-in	–	11898.27800	4,5	Normal (M)	11897.85	7.63	0.43 → 0.75	F 1	✓
S7384	74-in	–	13234.64681	4	Normal (S)	13234.20	0.78	0.45 → 0.48	1	–
S3416	40-in	–	5967.55248	2	Normal (M)	5967.00	1.19	0.55 → 0.60	1	✓
S6528	74-in	–	12520.21754	4	Normal (L)	12519.65	10.20	0.57 → 0.99	1 2	–
S5248	40-in	–	8202.36304	4,5	Normal (M)	8201.75	4.66	0.61 → 0.81	1	–
S0019	20-in	–	1573.44068	5	Normal (L)	1572.75	4.30	0.69 → 0.87	1 2	✓
S2623	40-in	–	3515.30484	4,5	Normal (M)	3514.60	3.60	0.70 → 0.85	1 2	✓
S7343	40-in	–	13155.65679	5	Normal (M)	13154.90	0.21	0.76 → 0.77	F 2	–
S0484	40-in	–	2023.30835	4	Super	2022.55	3.91	0.76 → 0.92	F 1	✓
S7222	74-in	B	13007.27570	4	Super	13006.40	7.54	0.88 → 1.19	1 2	✓
S0129	40-in	–	1691.29620	5	Super	1690.20	1.86	1.10 → 1.18	F	–
S7368	74-in	–	13169.48671	4	Normal (M)	13168.35	2.42	1.14 → 1.24	F 2	✓
S7301	40-in	–	13087.24153	5	Normal (M)	13086.10	2.94	1.14 → 1.26	2	✓
S1322	40-in	–	2355.38508	4	Normal (M)	2354.20	4.91	1.19 → 1.39	2	✓

* The time $T = 0$ is based on a template light curve of VW Hyi as defined in Paper I (see figure 5 of Paper I).

** F: Fundamental, 1: First harmonic, 2: Second harmonic. † S = short, M = medium, L = long.

ture and profile-fitted photometry using the DoPhot routine (Schechter, Mateo & Saha 1993). For a bright star such as VW Hyi, aperture photometry results in the highest signal-to-noise light curve. The lack of a suitably bright reference star near VW Hyi in the (small) field of view of the UCT CCD – $50'' \times 34''$ on the 74-in, and $109'' \times 74''$ on the 40-in reflector, respectively – means that all data presented here were obtained in clear conditions.

2.1 The Behaviour of the DNOs

2.1.1 The period evolution and appearance of harmonics

We have made Fourier transforms (FTs) of the VW Hyi light curves, in general following the progress of DNOs by dividing individual runs into subsections. These subsections range in length between ~ 5 minutes to ~ 1 hour (see Column 3 of Table 2). Within each subsection, we determined the DNO period, its formal uncertainty, and the amplitude of the modulation by a non-linear least-squares fit to the data. Even though the DNOs are generally not directly visible in the light curves, the signal in the FT is obvious and persistent and often marks the most prominent peak in the FT at high contrast with respect to the noise level (see Fig. 2). The identification of further harmonic signals (at exact multiple frequencies) can subsequently be done at greater sensitivity. Note, however, that we will only detect DNOs that are moderately coherent. The quantitative results are given in Table 2, but it is important to note that because the DNO period and amplitude are generally changing, the FT de-

fects only the sections of light curve that have relatively strong signals – we will later use amplitude/phase diagrams to produce greater sensitivity. Table 2 contains a considerable amount of data. As we are dealing here with a previously unobserved phenomenon in dwarf novae we consider it important to provide the evidence and uncertainties in some detail.

The over all behaviour is displayed in Fig. 1. The latter uses an abscissa on which time T is measured in days before or after a selected point near the end of the outburst decay light curve where all the light curves coincide; this is defined in Paper I. This enables us to place all the DNO evolutions on the same diagram; we estimate that the uncertainty in such timing (which arises almost entirely in fitting the observed light curve to the standard outburst templates: see Paper I) is ± 0.05 d. We have omitted most of the slow increase of P_{DNO} before $T = 0$, which is given in Paper I and is typical of the dP_{DNO}/dt seen in dwarf novae in general. The horizontal dashed line at $P_{DNO} = 14.1$ s shows the minimum value reached at maximum of outburst.

Discussing first the results from the FT analyses, which are biased towards the stronger signals but show the gross trends, we see that from $T = 0$ to $T = 0.20$ d there is a monotonic single-valued increase in P_{DNO} from 25 s to 33 s, as already seen in Paper I but now with additional data. At $T = 0.20$ d the first runs appear in which a 1st harmonic is sometimes present, but only at $T = 0.25$ d does the 1st harmonic dominate over the fundamental. The apparent turn-up in the trend of the fundamental in its last few points may be due to the unrecognised presence of syn-

Table 2. DNOs and QPOs in VW Hyi during decline from normal and super outburst.

Run No.	$\langle T \rangle$ (d)	Length (s)	DNOs (periods in seconds) [amplitude in mmag]			QPOs (period in seconds) [amplitude in mmag]		
			Fundamental	First harmonic	Second harmonic			
S0018	-0.21	3105*	20.22 ± 0.02	[2.2]	-	-	-	
	-0.19	3455*	20.28 ± 0.02	[2.2]	-	-	-	
	-0.18	2176*	20.55 ± 0.03	[2.2]	-	-	-	
	-0.17	448	20.70 ± 0.15	[4.3]	-	-	-	
S6133	-0.14	2418	19.84 ± 0.02	[1.8]	-	-	-	
	-0.11	3576	20.31 ± 0.02	[1.4]	-	-	-	
S6184	0.03	598	24.68 ± 0.09	[16.2]	-	-	-	
	0.04	861	24.73 ± 0.10	[8.6]	-	-	-	
	0.05	345	25.05 ± 0.22	[14.2]	-	-	-	
	0.05	1039	25.11 ± 0.05	[14.7]	-	-	-	
	0.06	343	25.22 ± 0.25	[9.7]	-	-	-	
	0.07	861	25.66 ± 0.09	[10.3]	-	-	-	
	0.08	343	26.33 ± 0.24	[12.4]	-	-	525 ± 4 [13.6]	
	0.08	519	26.22 ± 0.14	[13.3]	-	-	-	
	0.09	519	27.09 ± 0.12	[13.6]	-	-	-	
S6059	0.08	981	26.44 ± 0.05	[13.3]	-	-	407 ± 2 [18.3]	
	0.09	976	26.90 ± 0.05	[14.7]	-	-	-	
	0.11	984	27.11 ± 0.05	[15.2]	-	-	-	
	0.12	1245	28.05 ± 0.05	[12.5]	-	-	442 ± 3 [20.7]	
	0.13	865	28.29 ± 0.11	[11.9]	-	-	-	
	0.14	1120	29.35 ± 0.13	[6.0]	-	-	430 ± 6 [18.6]	
	0.16	1125	29.30 ± 0.06	[12.8]	-	-	-	
	0.17	1032	30.18 ± 0.07	[10.8]	-	-	-	
	0.18	1057	30.55 ± 0.06	[14.6]	-	-	463 ± 6 [14.0]	
	0.20	1208	31.34 ± 0.07	[11.8]	-	-	-	
	0.21	908	32.18 ± 0.11	[12.9]	-	-	-	
	0.22	912	32.89 ± 0.11	[12.1]	-	-	-	
	0.23	460	34.11 ± 0.26	[10.9]	-	-	578 ± 10 [22.5]	
	0.24	1124	34.75 ± 0.14	[9.8]	-	-	-	
0.25	949	36.57 ± 0.12	[15.0]	-	-	-		
0.27	546	38.60 ± 0.25	[17.1]	-	-	285 ± 4 [13.9]		
0.27	224	39.43 ± 1.26	[14.0]	-	-	-		
S0127	0.11	2592*	27.94 ± 0.03	[8.8]	-	-	-	
	0.12	2592*	28.64 ± 0.05	[5.5]	-	-	-	
	0.14	2592*	29.29 ± 0.04	[7.3]	-	-	-	
	0.15	2592*	29.72 ± 0.06	[7.8]	-	-	452 ± 5 [19.6]	
	0.17	2592*	30.15 ± 0.03	[9.2]	-	-	-	
	0.18	2592*	30.39 ± 0.04	[7.1]	-	-	-	
	0.20	2592*	32.09 ± 0.06	[5.9]	-	-	-	
	0.21	2592*	32.14 ± 0.05	[9.4]	-	-	443 ± 4 [22.3]	
	0.23	2592*	32.94 ± 0.07	[7.1]	-	-	492 ± 4 [27.8]	
	0.24	1900*	34.24 ± 0.08	[8.9]	-	-	-	
0.25	604	34.33 ± 0.14	[13.8]	-	-	-		
S7621	0.13	1200	26.55 ± 0.07	[9.8]	-	-	-	
	0.15	1200	27.22 ± 0.05	[11.0]	-	-	-	
	0.16	1200	28.28 ± 0.05	[10.7]	-	-	425 ± 2 [11.2]	
	0.17	1200	30.13 ± 0.05	[3.8]	-	-	-	
	0.19	1200	29.22 ± 0.05	[12.1]	-	-	-	
	0.20	1200	30.42 ± 0.05	[11.1]	-	-	-	
	0.22	1200	31.73 ± 0.05	[7.4]	-	-	-	
	0.23	1200	31.55 ± 0.05	[4.9]	-	-	-	
	0.24	1200	38.88 ± 0.05	[5.9]	-	-	-	
	0.26	1200	38.22 ± 0.05	[8.1]	-	-	-	
	0.27	600	-	-	18.32 ± 0.09	[4.9]	-	-
S2915	0.21	948	-	-	20.57 ± 0.08	[8.9]	-	-
S1307	0.21	600	-	-	18.15 ± 0.08	[5.0]	198 ± 2 [4.4]	
	0.22	1032	-	-	18.16 ± 0.04	[3.9]	-	

* This section includes a 50% overlap with the subsequent section.

Table 2. Continued: DNOs and QPOs in VW Hyi during decline from normal and super outburst.

Run No.	$\langle T \rangle$ (d)	Length (s)	DNOs (periods in seconds) [amplitude in mmag]			QPOs (period in seconds) [amplitude in mmag]		
			Fundamental	First harmonic	Second harmonic			
S7311	0.25	2000	–	–	–	399 ± 4	[9.9]	
	0.27	1036	–	19.57 ± 0.04	[6.2]	–	–	
	0.29	2333	–	19.93 ± 0.01	[6.1]	–	–	
	0.31	692	–	20.38 ± 0.11	[3.8]	–	–	
	0.32	1512	–	20.27 ± 0.02	[8.6]	–	298 ± 4 [10.1]	
	0.35	3241	–	20.75 ± 0.01	[7.7]	–	–	
	0.38	1900	–	21.05 ± 0.01	[14.0]	–	–	
	0.39	432	–	–	14.77 ± 0.08	[8.6]	–	
	0.40	1124	–	21.37 ± 0.05	[10.4]	–	351 ± 6 [8.7]	
	0.41	1036	–	21.85 ± 0.04	[11.5]	14.56 ± 0.04	[5.5]	–
	0.42	504	–	22.01 ± 0.07	[22.2]	–	657 ± 3 [6.6]	
	0.43	1384	–	22.71 ± 0.02	[15.2]	–	–	
	0.45	432	–	21.96 ± 0.09	[16.6]	–	–	
	0.46	1480	–	23.13 ± 0.02	[12.0]	–	–	
S7342	0.30	1576	–	20.94 ± 0.04	[3.6]	–	254 ± 2 [9.4]	
	0.31	780	–	19.85 ± 0.07	[7.4]	–	–	
	0.32	690	–	20.24 ± 0.09	[6.0]	–	–	
	0.33	780	–	20.73 ± 0.04	[9.8]	–	–	
	0.34	1230	–	19.82 ± 0.04	[5.2]	–	262 ± 5 [9.5]	
	0.36	565	–	20.40 ± 0.07	[11.3]	–	–	
	0.37	990	38.28 ± 0.15	[4.3]	20.86 ± 0.03	[11.7]	13.69 ± 0.04	[4.1]
	0.39	2250	–	21.20 ± 0.02	[7.7]	–	–	
0.41	1195	–	21.82 ± 0.04	[11.0]	–	–		
S6316	0.29	951	–	19.92 ± 0.04	[6.4]	–	–	
	0.30	995	–	20.47 ± 0.05	[7.0]	–	–	
	0.31	950	–	20.06 ± 0.04	[7.0]	–	–	
	0.33	1470	–	20.33 ± 0.03	[6.8]	–	–	
	0.34	950	–	20.62 ± 0.09	[3.9]	–	–	
	0.37	1555	–	20.87 ± 0.03	[7.7]	–	–	
	0.38	430	–	21.20 ± 0.09	[12.0]	–	–	
	0.38	650	–	21.86 ± 0.13	[6.3]	–	–	
	0.40	1424	–	21.74 ± 0.03	[9.1]	–	226 ± 2 [11.6]	
	0.41	950	–	22.18 ± 0.04	[9.4]	–	–	
	0.43	3283	–	22.56 ± 0.03	[2.1]	–	–	
	0.47	950	–	23.04 ± 0.05	[8.6]	–	–	
	0.47	560	–	23.56 ± 0.17	[6.1]	–	–	
	0.48	1081	–	23.77 ± 0.05	[10.0]	–	–	
0.50	1555	–	23.56 ± 0.06	[4.0]	–	231 ± 2 [9.2]		
0.52	1450	–	25.49 ± 0.07	[5.4]	–	–		
S6138	0.49	1516	–	25.31 ± 0.06	[6.8]	–	285 ± 4 [28.3]	
	0.52	1474	–	26.70 ± 0.09	[7.9]	–	–	
	0.53	437	–	29.58 ± 0.29	[11.4]	–	615 ± 2 [26.0]	
	0.54	1209	–	25.77 ± 0.09	[8.9]	–	–	
	0.57	2977	61.05 ± 0.17	[10.7]	–	–	–	
	0.61	1690	–	29.16 ± 0.08	[7.5]	–	–	
	0.63	1042	–	29.92 ± 0.18	[7.8]	–	–	
	0.65	2295	–	30.66 ± 0.07	[7.1]	–	350 ± 3 [30.6]	
	0.68	610	–	31.16 ± 0.21	[11.6]	–	–	
	0.70	1517	–	30.49 ± 0.06	[9.8]	–	–	
	0.72	1128	68.04 ± 0.83	[8.8]	30.13 ± 0.12	[12.3]	–	384 ± 2 [31.1]
	0.73	955	–	34.78 ± 0.28	[6.9]	–	768 (subharm.)	
	S7384	0.46	2108	–	26.76 ± 0.05	[6.4]	–	–
S3416	0.56	478	–	25.50 ± 0.21	[8.4]	–	–	
	0.56	346	–	24.19 ± 0.31	[12.1]	–	333 ± 2 [28.4]	
	0.57	431	–	26.96 ± 0.12	[17.6]	–	–	
	0.58	736	–	29.07 ± 0.19	[9.2]	–	–	
	0.59	492	–	29.75 ± 0.12	[16.6]	–	–	
	0.59	492	–	25.36 ± 0.22	[10.2]	–	–	
	0.60	384	–	25.91 ± 0.21	[16.4]	–	–	

Table 2. Continued: DNOs and QPOs in VW Hyi during decline from normal and super outburst.

Run No.	$\langle T \rangle$ (d)	Length (s)	DNOs (periods in seconds) [amplitude in mmag]			QPOs (period in seconds) [amplitude in mmag]	
			Fundamental	First harmonic	Second harmonic		
S6528	0.60	1904	–	–	18.81 ± 0.03 [6.0]	–	
	0.68	1728	–	–	20.81 ± 0.05 [3.4]	–	
	0.69	476	–	–	20.60 ± 0.19 [5.4]	–	
	0.70	905	–	–	21.20 ± 0.08 [5.0]	–	
	0.73	2028	–	–	22.56 ± 0.07 [3.1]	–	
	0.75	932	–	–	23.04 ± 0.12 [4.0]	–	
	0.84	932	–	–	24.13 ± 0.07 [5.7]	–	
	0.90	864	–	35.32 ± 0.39 [4.2]	23.53 ± 0.12 [5.9]	–	
	0.93	1249	–	37.29 ± 0.28 [3.8]	24.12 ± 0.12 [3.6]	–	
0.98	1573	–	–	26.09 ± 0.10 [3.0]	–		
S5248	0.63	3455	–	36.53 ± 0.09 [17.8]	–	–	
S0019	0.70	1242	–	29.90 ± 0.14 [9.9]	–	514 ± 2 [35.5]	
	0.71	1035	–	31.48 ± 0.12 [16.4]	–		
	0.72	520	–	29.76 ± 0.19 [21.0]	–		
	0.74	995	–	31.42 ± 0.18 [10.2]	–		
	0.77	1340	–	33.39 ± 0.13 [11.8]	21.83 ± 0.09 [7.8]		
	0.81	865	–	32.68 ± 0.20 [11.0]	–		
	0.82	690	–	35.68 ± 0.31 [12.2]	–		
	0.83	865	–	32.40 ± 0.25 [11.4]	–		
	0.84	1125	–	34.27 ± 0.16 [13.3]	–		
0.86	1725	–	32.65 ± 0.10 [12.2]	–	–		
S2623	0.71	928	–	–	23.55 ± 0.07 [12.9]	948 ± 5 [18.4]	
	0.72	730	–	–	21.81 ± 0.07 [18.5]		
	0.73	1015	–	–	25.36 ± 0.09 [9.3]		
	0.74	450	–	–	23.63 ± 0.07 [18.8]		
	0.75	1230	–	–	25.80 ± 0.06 [10.6]		
	0.76	760	–	36.93 ± 0.45 [5.0]	24.35 ± 0.08 [11.0]		
	0.77	585	–	–	24.95 ± 0.11 [12.0]		
	0.78	1660	–	–	22.48 ± 0.10 [6.1]		
	0.80	1640	–	–	23.38 ± 0.03 [15.1]		
0.82	2075	–	–	25.92 ± 0.03 [8.8]	256 ± 1 [12.6]		
0.84	1895	–	–	27.27 ± 0.05 [9.2]			
S7343	0.76	750	80.97 ± 0.30 [8.5]	–	26.45 ± 0.12 [8.9]	–	
S0484	0.77	1396	–	33.25 ± 0.15 [5.5]	–	457 ± 3 [31.8]	
	0.80	1816	–	33.72 ± 0.14 [6.2]	–		
	0.82	1380	–	39.48 ± 0.41 [3.9]	–		
	0.83	1288	–	37.81 ± 0.34 [3.6]	–		
	0.84	608	–	34.21 ± 0.28 [7.9]	–		
	0.86	520	–	29.43 ± 0.45 [8.7]	–		
	0.87	196	66.93 ± 2.78 [12.4]	–	–		1328 ± 2 [44.1]
	0.88	780	–	44.31 ± 0.63 [7.6]	–		
	0.89	732	–	34.51 ± 0.27 [6.3]	–		530 ± 4 [36.1]
	0.91	692	–	30.92 ± 0.30 [6.3]	–		
0.91	388	–	35.44 ± 0.49 [8.6]	–			
0.92	604	–	32.69 ± 0.41 [6.3]	–			
S7222	0.88	790	–	–	26.34 ± 0.14 [8.8]	–	
	0.89	584	–	–	27.47 ± 0.18 [10.3]	–	
	0.90	1380	–	–	26.30 ± 0.12 [5.3]	–	
	0.93	948	–	–	27.59 ± 0.11 [7.5]	–	
	0.93	288	–	–	25.08 ± 0.20 [7.5]	–	
	0.94	432	–	–	26.99 ± 0.34 [6.2]	–	
	0.94	432	–	–	24.68 ± 0.20 [7.7]	–	
	0.95	608	–	–	26.34 ± 0.20 [7.1]	–	
	0.96	688	–	–	27.12 ± 0.18 [5.2]	–	
	0.97	1184	–	–	29.51 ± 0.11 [7.9]	271 ± 4 [11.9]	
	0.98	1152	–	–	30.08 ± 0.12 [7.6]		
	0.99	944	–	38.24 ± 0.25 [7.3]	–		
1.00	908	–	–	30.25 ± 0.18 [10.3]			
1.01	992	–	–	32.15 ± 0.24 [6.7]	–		

Table 2. Continued: DNOs and QPOs in VW Hyi during decline from normal and super outburst.

Run No.	$\langle T \rangle$ (d)	Length (s)	DNOs (periods in seconds) [amplitude in mmag]			QPOs (period in seconds) [amplitude in mmag]
			Fundamental	First harmonic	Second harmonic	
S7222	1.02	348	–	–	31.25 ± 0.37 [10.9]	–
	1.03	656	–	–	30.88 ± 0.24 [6.2]	–
	1.08	1036	–	–	33.84 ± 0.14 [9.6]	–
	1.10	1467	–	–	29.41 ± 0.10 [6.8]	306 ± 2 [23.4]
	1.13	864	–	–	27.86 ± 0.19 [8.1]	–
	1.14	1081	–	–	29.25 ± 0.19 [8.9]	–
			–	–	34.36 ± 0.28 [8.2]	–
	1.15	1380	–	–	28.56 ± 0.15 [6.2]	–
	1.17	1728	–	–	33.88 ± 0.14 [5.8]	–
S0129	1.13	3885	93.15 ± 0.29 [16.1]	–	–	–
S7368	1.14	800	90.49 ± 1.23 [8.2]	–	30.23 ± 0.16 [7.0]	321 ± 3 [24.5]
	1.15	573	–	–	31.11 ± 0.23 [9.2]	
S7301	1.14	520	–	–	30.19 ± 0.31 [7.6]	–
	1.15	475	–	–	31.26 ± 0.42 [7.6]	–
	1.16	430	–	–	33.08 ± 0.34 [8.1]	–
	1.18	775	–	–	32.62 ± 0.31 [8.5]	–
	1.20	1165	–	–	33.19 ± 0.29 [6.2]	–
	1.22	910	–	–	30.13 ± 0.24 [8.4]	–
	1.23	735	–	–	31.99 ± 0.40 [5.0]	–
	1.24	690	–	–	35.04 ± 0.36 [6.3]	–
	1.25	1210	–	–	32.78 ± 0.20 [5.9]	–
	1.26	935	–	–	31.85 ± 0.16 [7.7]	–
	1.31	635	–	–	32.68 ± 0.28 [7.5]	–
	1.41	7236	–	–	–	581 ± 2 [19.0]
	S1322	1.24	880	–	–	29.21 ± 0.11 [13.8]
1.25		348	–	–	33.29 ± 0.37 [11.0]	–
1.27		2072	–	–	29.34 ± 0.08 [6.8]	–
1.30		520	–	–	28.41 ± 0.29 [8.9]	–
1.31		1036	–	–	31.66 ± 0.13 [8.0]	–
1.34		656	–	–	29.66 ± 0.17 [18.2]	424 ± 1 [29.7]
1.35		944	–	–	28.52 ± 0.16 [11.2]	
1.36		648	–	–	31.22 ± 0.19 [13.4]	
1.37		404	–	–	25.85 ± 0.19 [20.0]	
1.37		804	–	–	28.68 ± 0.16 [8.3]	
1.38		484	–	–	31.75 ± 0.23 [14.2]	–
1.39	468	–	–	32.15 ± 0.29 [12.4]	–	

odic rather than direct DNOs, but we see no evidence for any double DNO in the observations at this stage (in the rare cases when we observed a double DNO at other times we have plotted only the direct period in Fig. 1).

From $T = 0.25$ to 0.50 the 1st harmonic increases in period with little scatter, but from $T = 0.36$ it is occasionally accompanied by a 2nd harmonic, which to our knowledge is the first such observation of frequency tripling in a CV.

From $T = 0.5$ to 1.0 d the evolution of the DNOs is characterised by increasing domination of the 2nd harmonic over the 1st, until at $T = 1.0$ only the 2nd harmonic is present and appears to stabilize at a period ~ 30 s, though with considerable scatter. For a day or so after $T = 1.4$ d, by which time VW Hyi is fully at quiescence, our light curves show no DNOs at all. On rare occasions through the $T = 0.25 - 1.1$ d range there are guest appearances of the fundamental.

In most of the runs after $T = 0.3$ d either the 1st or the 2nd harmonic is present, and there is alternation between them within the run, but in runs S6138 and S7342 there

are parts where fundamental and both harmonics are simultaneously present in the FTs; these are shown in the inset in Fig. 1. Our FTs show that the 1:2:3 ratios of periods are satisfied within errors of measurement when the components are present together. In Fig. 2 we illustrate FTs that contain combinations of the fundamental, 2nd and 3rd harmonics present simultaneously (because one or other component usually dominates, the presence of the weaker components is usually only made convincing by inspecting FTs of the immediately preceding or subsequent sections of the runs, where they in turn may dominate).

In Fig. 1 the dotted and dashed lines are least squares fits to the 1st and 2nd harmonics (with all parameters free, but omitting the 2nd harmonic points with $T > 1.15$ d) and appear again in the upper part of the diagram multiplied by two and three respectively to show the approximate evolution of the implied fundamental.

Fig. 3 shows a modified form of Fig. 1, where we have now transformed the 1st and 2nd harmonics into the implied fundamental to show its evolution more clearly. This shows

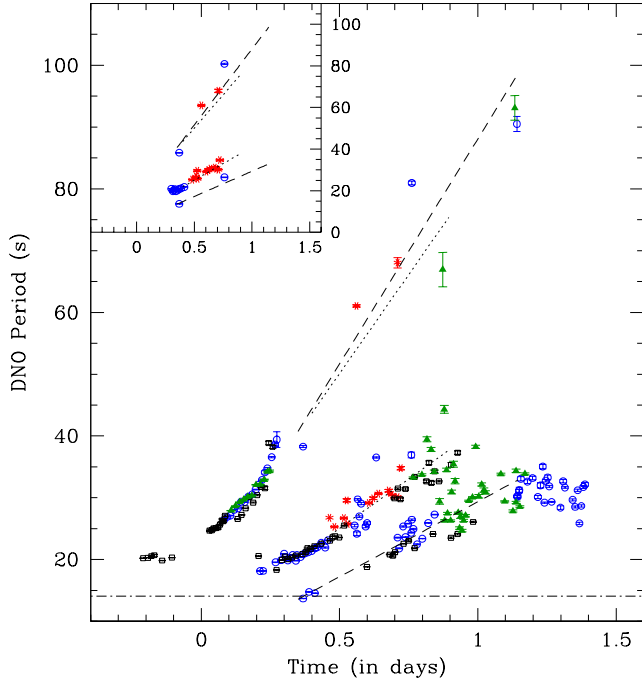


Figure 1. The evolution of DNO periods at the end of normal and super outbursts in the dwarf nova VW Hyi. The different symbols indicate the different kind of outbursts (short: asterisk, normal: open circles, long: open squares and super outbursts: filled triangles). The dotted and dashed lines show the result of the least squares fit to the first and second harmonic, respectively, and are multiplied by a factor of two and three to show the evolution of the fundamental DNO period. The horizontal dotted-dashed line illustrates the minimum DNO period (14.1 s) observed at maximum brightness. The inset highlights two observing runs in which the fundamental, first and second harmonic of the DNO period were occasionally present simultaneously.

that the fundamental systematically increases in period to ~ 105 s before the DNOs disappear completely. When passing through 85 – 95 s any appearance of the fundamental in the FT may be confused with the lpDNOs in VW Hyi that occur in that period range. However, the lpDNOs observed so far (in VW Hyi and other CVs) are all pure sinusoids and often long-lasting, so most of them can be recognised for what they are and have been omitted from Fig. 1. In VW Hyi it therefore appears that at times the fundamental period of the normal DNOs can briefly reach values greater than the period of the lpDNOs, but the tendency for the 2nd harmonic to stabilize near ~ 30 s at the end of the whole DNO evolution is a strong indication that $P_{DNO} \rightarrow P_{lpDNO}$ at the end of outburst.

The dashed line in Fig. 3 is the least squares fit for $T = 0.2$ to 1.15 d and has the equation

$$P_{DNO}(s) = 65.06 (\pm 1.49) T(d) + 19.0 (\pm 1.0). \quad (1)$$

The formal errors on the parameters derived from the least squares fit are given in Eq. 1 in brackets.

2.1.2 Some details of the DNO behaviour

In order to obtain greater sensitivity to the fast changing periods we have calculated amplitude and O–C values, fitting

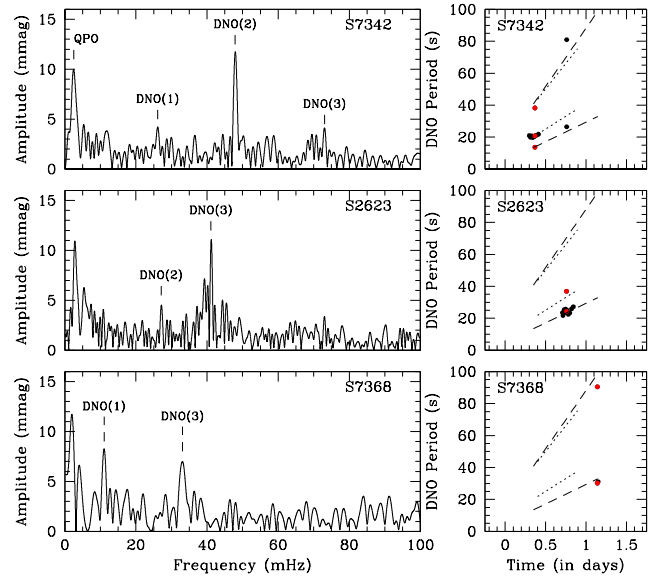


Figure 2. Examples of parts of runs where there are harmonics simultaneously present. The left panels show selected Fourier transforms from three observing runs (S7342, S2623, S7368, respectively, from top to bottom); prominent peaks are marked and labelled. The right panels show a small version of Fig. 1 for the three runs displayed here.

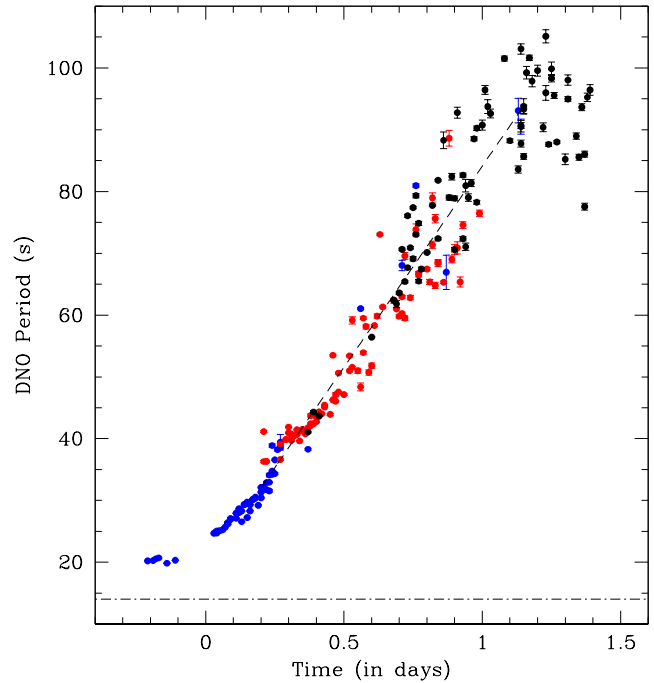


Figure 3. Time evolution of the observed or implied fundamental DNO period.

sinusoids by least squares to short and usually overlapping sections of the light curves. These are amplitude/phase diagrams, which we will call A/ϕ plots. Here we will show a few of the more significant ones.

The FT of run S6316 contains only 1st harmonic DNOs and S7311 is predominantly 1st harmonic. In order to compare their behaviour with that of the fundamental (which

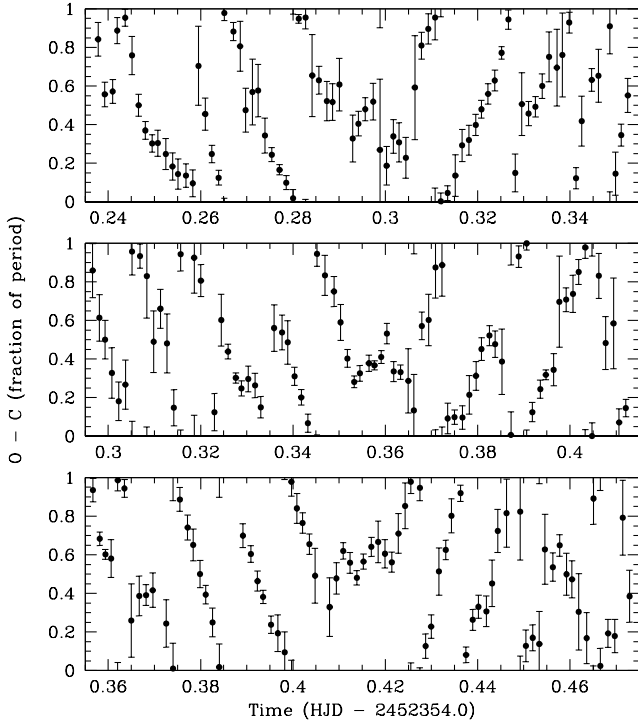


Figure 4. Phase diagram for the first harmonic component of DNOs in run S6316. The three panels are for the first half (relative to $P_{DNO} = 20.62$ s), the centre half (22.18 s), and the final half (23.04 s) of the run. The phases ‘wrap around’ if they exceed one period.

would have been strongly present only an hour or so before the start of these runs – as seen in S6059 in Table 2) we give in Figs. 4 and 5 phase diagrams structured in the same manner as the ‘oak panel diagram’ of S6059 shown in figure 10 of Paper I. These show that the general behaviour of fundamental and 1st harmonic DNOs are essentially identical: short-lived increases and decreases of period or phase superposed on the steady increase in mean period. S7311 is, however, relatively more coherent than S6316, with smaller deviations from the secular increase in period.

Run S6138 is predominantly 1st harmonic and is the first to show noticeable scatter in period. To examine this at greater resolution we give a phase diagram in Fig. 6, where the run has been divided into two equal parts and the phases are measured relative to periods 25.77 s and 30.50 s respectively. In the upper panel there is the quasi-parabolic variation with phase changing by several cycles, which is the signature of a steadily increasing period, but in the lower panel there is variation (with a range \sim one cycle) around a constant phase, showing no systematic increase in period over the 3.7 h span of time. There is no noticeable difference in the gross light curve behaviour between the two halves of the run (the second half of which is shown in figure 2 of Paper II), but we note that optical flux is largely determined by accretion in the outer parts of the disc, whereas the evident temporary relative stability of P_{DNO} and its implied \dot{M} is a property of the inner disc.

Towards the end of run S6528, which again is largely 2nd harmonic, the FTs show occasional detectable presence of the 1st harmonic (see Table 2). We use this run to demon-

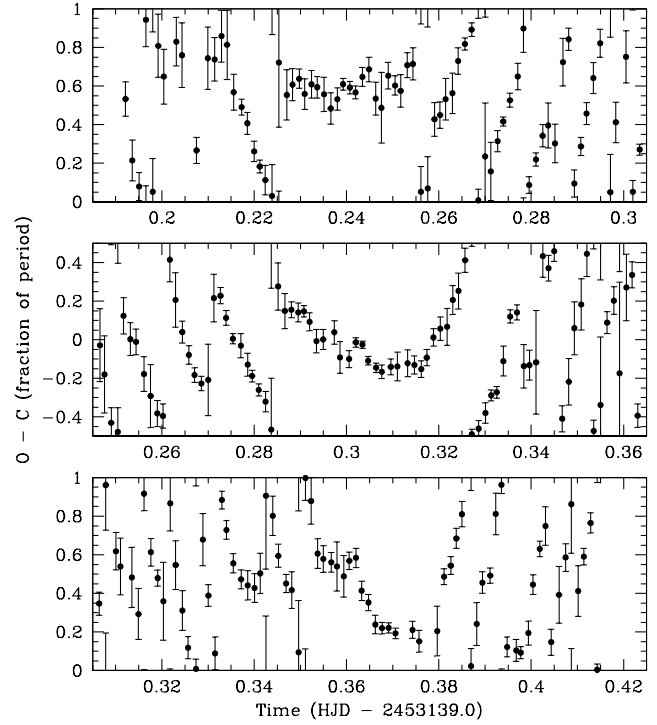


Figure 5. As for Fig. 4, but for run S7311. The phase diagrams are plotted relative to a DNO period of 19.93 s (top), 20.75 s (middle) and 22.01 s (bottom), respectively.

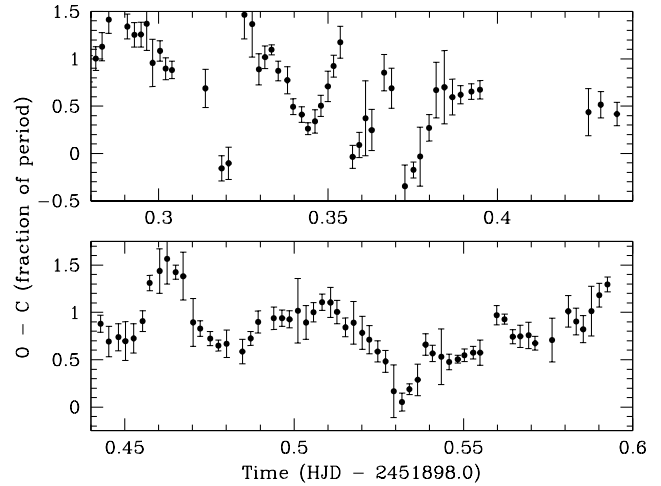


Figure 6. Phase variations of the first harmonic in run S6138.

strate the importance of not relying on FTs alone. The bottom panel of Fig. 7 shows the A/ϕ diagram for the 2nd harmonic, relative to a test sinusoid with period 23.94 s, which we have smoothed and reduced the uncertainties by using longer sections of light curve. Despite the low amplitude of the signal, the smoothly varying phase measurements show that the 2nd harmonic is almost always present. The middle panel shows the A/ϕ diagram for the 1st harmonic, using a test sinusoid of period $\frac{3}{2} \times 23.94 = 35.91$ s, where it can be seen that the 1st harmonic is also almost always present, but its phase variations are not obviously positively or negatively

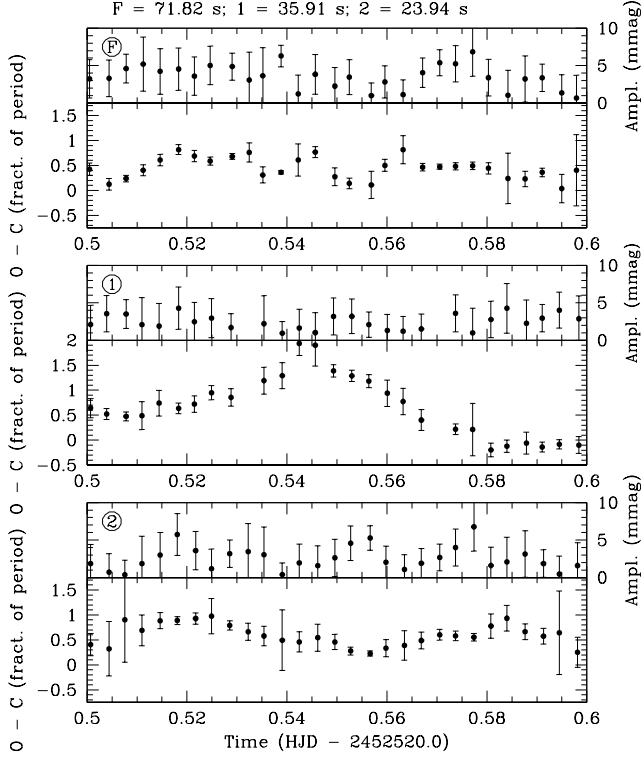


Figure 7. Phase and amplitude variations of the fundamental (top), first harmonic (middle) and second harmonic (bottom) in run S6528.

correlated with those of the 2nd harmonic; this means, of course, that they do not maintain an exact 2:3 period ratio, but nor do they drift apart in any systematic way. Finally, in the top panel of Fig. 7 we show the result of searching for the presence of the fundamental, using $3 \times 23.94 = 71.82$ s as the comparison period. This reveals that, despite there being no clear peak in the FT near 71.82 s (which is a region of increased noise at the lower frequency end of CVs in general), there is a low amplitude fundamental almost continuously present, with well-defined phase that appears to follow the variation of the 2nd harmonic.

We have investigated sections of other runs where the periods stay almost constant for considerable lengths of time – these give similar impressions to what we have found in run S6528, but with less certainty because of smaller amplitudes.

There remains to show what DNO components can be discerned when the period is changing rapidly. We analyse two runs as exemplars. First we look again at run S6316, for which Fig. 4 gives the oak panel diagram of the 1st harmonic. In Fig. 8 the first half of the run is shown, giving both A and ϕ in the lower panel, relative to a sinusoid of period 20.62 s but using longer sections of light curve to provide a smoother version of the top panel of Fig. 4. The upper panel of Fig. 8 shows the result of least squares fits in the neighbourhood of the implied fundamental (i.e., using a test period of 41.24 s). It is seen that the fundamental is continually present, albeit of very low amplitude, and that it has a ‘parabolic’ phase variation similar to that of the 1st harmonic (note that because the period is double, the total phase variation of the fundamental is half that of the 1st harmonic).

Lastly we look at run S7311, which is the first run af-

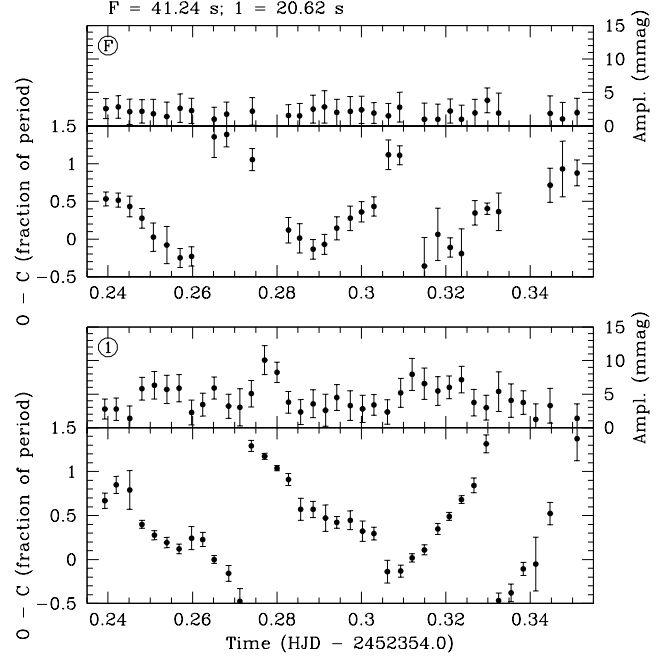


Figure 8. Phase and amplitude variations of the implied fundamental (top), and observed first harmonic (bottom) in run S6316.

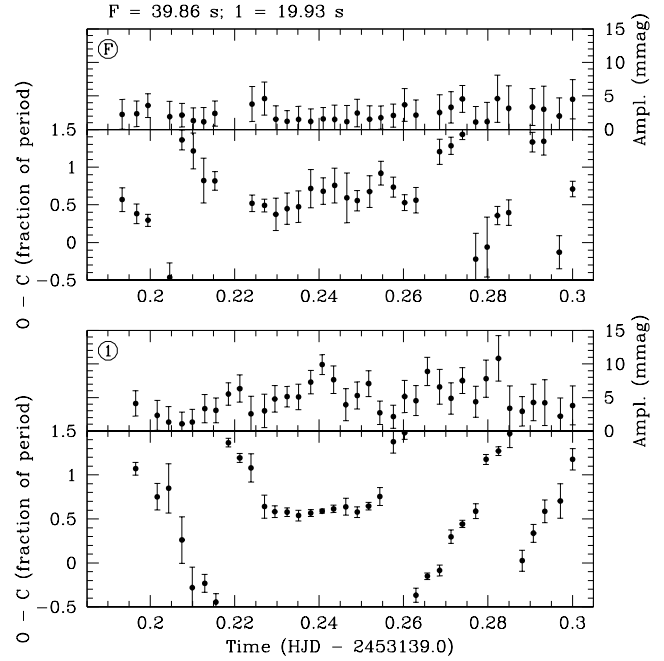


Figure 9. Phase and amplitude variations of the implied fundamental (top), and observed first harmonic (bottom) in run S7311.

ter the fundamental has disappeared and the 1st harmonic is strong (see Fig. 1). In Fig. 9 the 1st harmonic shows a parabolic phase change and there is a low amplitude fundamental with the same behaviour. On the other hand, the 2nd harmonic does not appear to be present – the amplitudes are very small and the phases spread over a full cycle and do not show the parabolic variation.

In summary, for small variation, the fundamental and

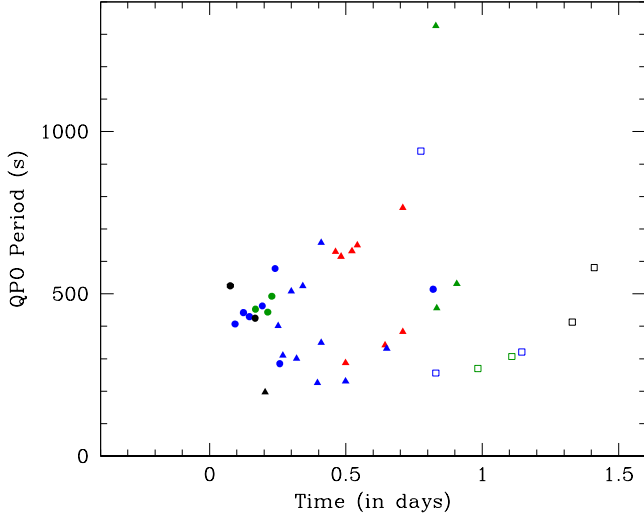


Figure 10. The evolution of QPO periods in the late decline of outbursts in VW Hyi. The filled circles indicate runs with the fundamental DNO period predominantly present, filled triangles represent runs where the first harmonic of the DNO period is dominant, and the open squares indicate runs where the second harmonic of the DNO is present.

2nd harmonic components follow each other in phase variation, but the 1st harmonic has an independent variation. For the more general steady increase in period the fundamental and harmonics follow each other as expected.

2.2 The Behaviour of the QPOs

We have analysed the QPO signals in the same way as for the DNOs. The QPOs are initially identified in the Fourier transform of subsections of data for each observing run; these subsections have typical data lengths of ~ 30 to ~ 45 minutes, corresponding to between ~ 5 and ~ 10 cycles of a QPO modulation. Given the incoherent nature of the QPOs and the presence of flickering on similar time-scales, QPOs are difficult to identify using standard techniques. Therefore, we have been fairly conservative in identifying the QPOs – only those that are then clearly seen in the light curves for at least several cycles are accepted. There are probably other short-lived QPOs, made difficult to identify because of stochastic flickering in the light curve. In Paper I we reported that the ~ 600 s QPOs in the February 2000 outburst of VW Hyi halved in period near the end of our run (see also Table 2). This was a first hint that we should expect frequency doubling in the QPOs, as observed in the DNOs. This has proved to be the case, and also extends to tripling of frequencies – our results are shown in Fig. 10 and the periods are listed in Table 2.

From Fig. 10 we see that the first appearance of the first harmonic of the QPOs is at $T = 0.2$ d, which is the same place at which the DNO 1st harmonic begins. The second harmonic starts at $T \sim 0.8$ d, which is where the DNO second harmonics begin to become very prominent. Again we can produce a modified plot, given in Fig. 11, in which we have shown the implied fundamental QPO periods. The solid line in Fig. 11 is a least squares fit to these points and has the equation, for the range $0.2 < T(d) < 1.15$,

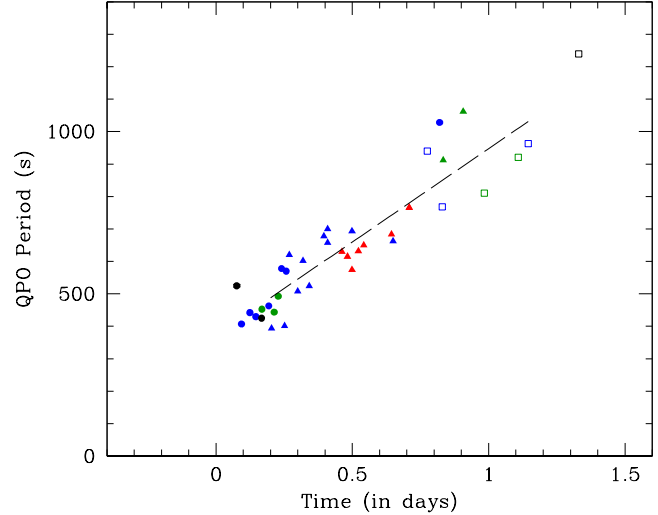


Figure 11. The evolution of the measured and implied fundamental QPO periods in VW Hyi. The symbols are as in Fig. 10 and the dashed line is a least squares fit to the data (see Eq. 2).

$$P_{QPO}(s) = 575 (\pm 54) T(d) + 372 (\pm 33), \quad (2)$$

where the formal errors on the parameters derived from the least squares fit are given in brackets in the above equation (Eq. 2).

Equations 1 and 2 show that the ratio R is not constant during the factor of three increase in fundamental period seen in VW Hyi. In fact, R changes from 15.2 at $T = 0.2$ d to 11.0 at $T = 1.15$ d, which is typical of the range of values seen among other CVs, e.g., Mauche (2002) found $R = 10.4$ and 11.4 for two runs on SS Cyg and in Paper III we found $R = 15$ for TU Men and V893 Sco. Values of R outside of this range may arise from unwittingly combining DNO and QPO fundamentals with harmonics.

3 INTERPRETATION

3.1 Introduction

In order to prepare for our suggested interpretation of the complicated behaviour of VW Hyi we recall some of the structural components that have been used to explain the rapid brightness modulations in CVs.

(i) DNOs seen at optical wavelengths have their origin in the reprocessing of harder radiation, emitted anisotropically from the accretion zone(s) near the primary, striking the primary or sweeping around the concave surface of the accretion disc. These generate a modulation at the rotation period of the accretion zone, P_{rot} . It is possible also to generate a signal at $\frac{1}{2}P_{rot}$: although the simplest model of a tilted concave disc generates a sinusoidal signal, with the far side and near side disc contributions being 180° out of phase and therefore giving an amplitude which is the difference of the two signals (Petterson 1980), more generally the two components may not be so completely sinusoidal. For example, if there were strong forward or backward scattering then the signal would have narrow peaks when the beam was pointing directly forward or away from us. Furthermore, the signals from the far side of the disc and from

the primary are 180° out of phase, which can generate two peaks per rotation. There may also be situations where two accretion zones are visible (to the disc or to us) which also produce what is in effect the 1st harmonic of the rotation period.

(ii) If the rotating beam intercepts a structure such as the secondary, or the thickened disc in the vicinity of the stream impact on the disc, which is revolving with the orbital period, then a modulation is generated at the ‘synodic’ period P_{syn} , obtained from $P_{syn}^{-1} = P_{rot}^{-1} - P_{orb}^{-1}$, which we can more compactly write in frequencies as $\omega_{syn} = \omega_{rot} - \Omega_{orb}$. This process is commonly present in intermediate polars and generates a single orbital sideband to the ω_{rot} signal.

(iii) If the reprocessing site is periodically modulated in cross section, this introduces an amplitude modulation into the reprocessed signal. As an example, suppose that the reprocessing site is most favourably placed just once per orbital period, this then generates sidebands to the ω_{syn} signal at $\omega_{syn} + \Omega_{orb}$ and $\omega_{syn} - \Omega_{orb}$, i.e. signals at ω_{rot} and $\omega_{rot} - 2\Omega_{orb}$, as well as the original $\omega_{rot} - \Omega_{orb}$ (see Warner (1986) for this and more complicated examples). The sideband signals, which would be of equal amplitude in the simplest case, are often unequal because of the presence of components generated by other mechanisms, which may be in or out of phase with them (and may be of variable amplitude).

(iv) If \dot{M} onto the primary is itself periodically modulated then sidebands to the ω_{rot} signal or any of the reprocessed signals may be generated. This is the ‘beat frequency’ model introduced first for CVs (Warner 1983), shown later not to work for the standard DNOs (Warner 1987), but independently invented and successfully applied to some types of QPOs in X-Ray Binaries (Alpar & Shaham 1985; Lamb et al. 1985), and used to interpret T Tauri light curves (Smith, Bonnell & Lewis 1995).

3.2 The DNO Frequency Doubling

There are at least two ways in which frequency doubling of DNOs might arise. Given the general structure of the LIMA model, one possibility is a transition from single-pole to two-pole accretion. This might be due simply to a change in the field-threading region as \dot{M} changes, resulting in feeding of two accretion zones instead of one. A transition to quadrupole field from dipole field configuration may occur when the inner edge of the accretion disc is pushed so close to the white dwarf surface that the less compressible higher order multipole field components determine the position of the inner edge of the disc (Lamb 1988); but in reverse this would reduce the number of accretion zones as \dot{M} decreases and is thus unlikely to be related to frequency doubling in VW Hyi late in outburst when \dot{M} is decreasing.

It is not easy to make quantitative predictions about the changes in magnetic field structure that would lead to the above effect, but another possibility is that frequency doubling arises through a geometrical rearrangement, which allows us (or the reprocessing regions of the accretion disc) to view two poles instead of one. The smoothness of the transition to a dominant doubled DNO frequency – in the sense that there is no concomitant apparent change in behaviour (coherence, jump to longer periods, amplitude) – suggests that no radical restructuring has occurred in the threading

region or in the accretion zones. We have therefore considered models in which either the upper accretion zone becomes visible as the inner edge of the accretion disc retreats outwards with decreasing \dot{M} , or the second accretion zone becomes visible. Such a transition is well documented in the case of the X-Ray light curve of the intermediate polar XY Ari (Hellier, Mukai & Beardmore 1997).

In Paper I we noted that the shortest observed P_{DNO} in VW Hyi is 14.1 s (seen only very rarely, but in both optical and X-Rays at the maxima of different outbursts). Interpreted as the period of Keplerian rotation at the surface of the primary (i.e. the minimum period that the innermost parts of the disc or the equatorial belt can have before magnetic channeling of gas ceases as the magnetosphere of the primary is crushed by the mass flow) this implies a primary mass $M(1) = 0.70 M_\odot$ and radius $R(1) = 7.79 \times 10^8$ cm from the Nauenberg (1972) mass-radius relationship for white dwarfs. From the large amplitude orbital humps but absence of eclipses in the light curve of VW Hyi it has long been assumed that the inclination is $\sim 60^\circ$. However, on 2 January 2004, towards the end of a superoutburst of VW Hyi, we observed what appear to be grazing eclipses of the bright spot, made possible by the increased size of the accretion disc as it expanded in response to the outward flow of angular momentum from the gas falling inwards. A similar effect has been seen in TY PsA (Haefner, Schoembs & Vogt 1979; Warner, O’Donoghue & Wargau 1989). We therefore use the slightly larger inclination of 64° .

In the LIMA model the accretion zones are within the equatorial band and will be long arcs, probably one somewhat above the equator and one below, on opposite sides of the primary. When the inner edge of the disc is close to the primary, the primary itself obscures the inner parts of the disc on the far side. As the inner radius r_{in} of the disc increases with decreasing \dot{M} in the final phase of an outburst, these inner regions, which contain the upper accretion curtain, come into view beyond the primary (and at the same time part of the accretion curtain feeding the second pole may become visible beyond the inner edge of the disc on the near side). This happens at $r_{in} \sim R(1) \sec i$. The Keplerian period of the inner edge of the disc is then found from

$$P_k^2 = 4\pi^2 R^3(1) \sec^3 i / GM(1), \quad (3)$$

which produces $46.2 \text{ s} < P_k < 51.4 \text{ s}$ for the range $63^\circ < i < 65^\circ$. We suggest, therefore, that for $P_{DNO} < P_k$ we view only the ‘upper’ accretion zone and curtain when it is on our side of the primary, but when $P_{DNO} > P_k$ we see that accretion curtain again when it is on the far side of the primary (where it may appear even brighter: Hellier et al. 1987); and there may also be a contribution from the lower accretion zone, both giving a double humped luminosity profile for each rotation of the equatorial belt. Any inequality of apparent luminosity of the two components will add a fundamental period to the 1st harmonic.

Frequency doubling should therefore occur near $P_{DNO} \sim 48 \text{ s}$, as is indeed observed.

We note also that frequency doubling of a synodic DNO can occur simply by a QPO traveling wave itself transforming to a double-humped profile, i.e. through excitation of the 1st harmonic.

3.3 The Appearance of a Second Harmonic

Frequency tripling is not a common physical phenomenon – in particular we think it very unlikely that in VW Hyi it could be the result of accretion onto three magnetic regions. We therefore consider a model in which the 2nd harmonic of the DNO fundamental does not represent a physical frequency in the VW Hyi system, but rather is, just as observed, a Fourier component of the light curve. The fact that the 2nd harmonic does not appear until the 1st harmonic is already present is in agreement with this hypothesis, though this cannot be a strict prerequisite because the 2nd harmonic on its own appears in many of the later light curves. When this happens it implies that there are other sources of fundamental and 1st harmonic signals that can be out of phase with the amplitude modulated components at those frequencies.

3.3.1 Beat Frequency from the Wall

Consider the state of VW Hyi nearing quiescence after outburst. The disc has a very low \dot{M} and will be thin in vertical extent. When the fundamental $P_{DNO} \sim 60$ s the inner disc has been emptied by the primary’s rotating magnetosphere out to $\sim 1 \times 10^9$ cm above the surface of the primary. The structure subtending the largest angular size that the rotating DNO beam can illuminate is the thickened part of the inner disc that generates the QPO modulation (we note here that QPOs are a common feature in these late stages of a VW Hyi outburst). The QPO traveling wave will also effectively block illumination by the DNO beam of a large area of the disc, but the disc will always be accessible to the beam during the half of the beam cycle that passes over the lower half of the wave profile. Depending on the relative strengths of these two components, the rapid oscillations seen in these late phases of outburst could at times be predominantly synodic DNOs rather than direct ones.

The postulated QPO wave is a region of disc thickening near the inner edge of the accretion disc. The strongest field lines, which will be the dominant collectors of gas from the disc, sweep past this thicker region[‡] with a frequency $\omega_{rot} - \omega_{qpo}$, where ω_{qpo} is the frequency of the traveling wave (typically about one fifteenth of ω_{rot} , unless frequency doubling has occurred in one of them). We therefore may expect the two accretion zones on the primary each to be modulated in luminosity at a frequency $\omega_{rot} - \omega_{qpo}$.

The result is that the 1st harmonic, generated either as a result of seeing one luminous zone twice per rotation, or two accretion zones separated in longitude by roughly 180° , is modulated in luminosity. For synodic DNOs the 1st harmonic has frequency $2(\omega_{rot} - \omega_{qpo})$ and the \dot{M} modulation frequency is $\omega_{rot} - \omega_{qpo}$. This will generate Fourier components that include sidebands at the sum and difference frequencies (see, e.g., Warner 1986), i.e. at $\omega_{rot} - \omega_{qpo}$, $2(\omega_{rot} - \omega_{qpo})$ and $3(\omega_{rot} - \omega_{qpo})$. As already mentioned

[‡] The region of disc thickening will not necessarily be where the mass transfer is highest – the thickest part of the wave might (because of mass continuity in the Keplerian flow) be a region of relative rarefaction and cause a lower rate of mass transfer. But in any case there is a periodic modulation of mass transfer as the field lines sweep around the inner edge of the disc.

above, there may be other mechanisms contributing to the brightness of the fundamental and/or the 1st harmonic components, which will alter the amplitudes of those components from the simple 1:2 ratio of amplitude modulation, but the 2nd harmonic is generated in our proposed model solely as a rotational sideband.

3.3.2 Beat Frequency from the Disc

Another possibility is that the traveling wall does not intercept much of the beam radiation, but the accretion rate is still modulated at frequency $\omega_{rot} - \omega_{qpo}$. The optical DNOs are then generated in the normal way off the disc. No longer are there precise harmonic ratios – we would see the frequency set $\omega_{rot} + \omega_{qpo}$, $2\omega_{rot}$ and $3\omega_{rot} - \omega_{qpo}$, which differ slightly from 1:2:3 ratios. We have not detected any convincing examples of such behaviour in our VW Hyi observations.

3.3.3 Combinations of the two Beat Frequency Models

The differences between the models can in principle be tested by looking at the period ratios for FTs where the fundamental and its apparent harmonics coexist. There is also the possibility of both processes acting simultaneously – with part of the beamed radiation coming from the disc and part from the wall. This would, from comparison of the frequencies generated in the two models, produce double DNOs in all components, with a frequency splitting of $2\omega_{qpo}$. This is different from the non-modulated mass transfer case, where the splitting is ω_{qpo} in the fundamental (Paper II).

In addition to these possibilities it may happen that there is no \dot{M} variation, so the fundamental and its first harmonic can be seen both at direct and synodic frequencies, i.e. double DNOs at ω_{rot} , $\omega_{rot} - \omega_{qpo}$ and/or at $2\omega_{rot}$ and $2(\omega_{rot} - \omega_{qpo})$.

Such simultaneous or alternating presence of the various options could account for part or all of the vertical scatter in Figs. 1 and 3. It is difficult to test for all of these effects simultaneously, but we may find some of these processes at work individually. We give two examples in detail, selected from regions in Fig. 1 where there are widely different P_{DNO} in contiguous subsections – in effect, double DNOs with the components separated in time.

Fig. 12 shows the A/ϕ diagram for a section of Run S7222, computed with the test period 27.0 s. The marked subsections I to IV have P_{DNO} values of 27.59, 25.08, 26.99 and 24.68 s respectively. The beat period between the periods in subsections I and II is 285 s, and that for subsections III and IV is 288 s. There is no QPO directly detectable in this section of the light curve (although the light curve is not particularly noisy at this time), but in the part almost immediately following, namely during 0.3750 – 0.3925 d, there is a strong QPO with a period of 271 ± 4 s. The effect in the A/ϕ diagram is, therefore, one that would be expected of alternating direct and synodic DNOs, where the DNO beam is reprocessed from a QPO traveling wave, but not of sufficient amplitude to produce QPOs as seen from our direction. After subsection IV in Fig. 12 there is no clear interpretation of the behaviour.

Fig. 13 is a section of run S6138, with the A/ϕ diagram

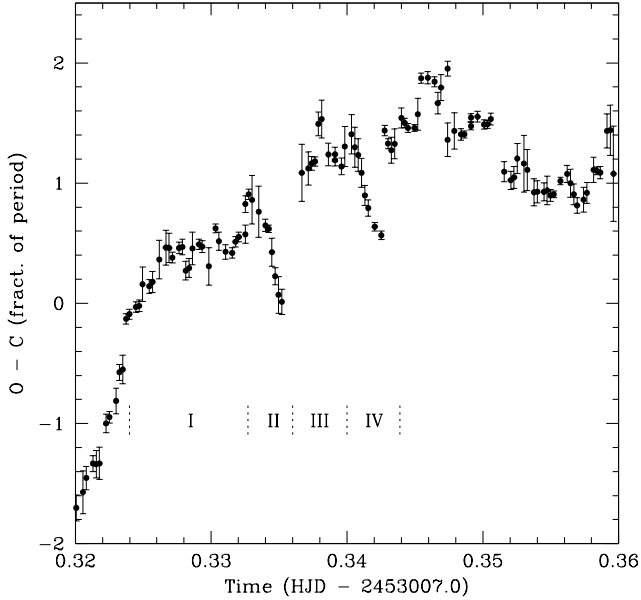


Figure 12. Phase variation in a section of run S7222.

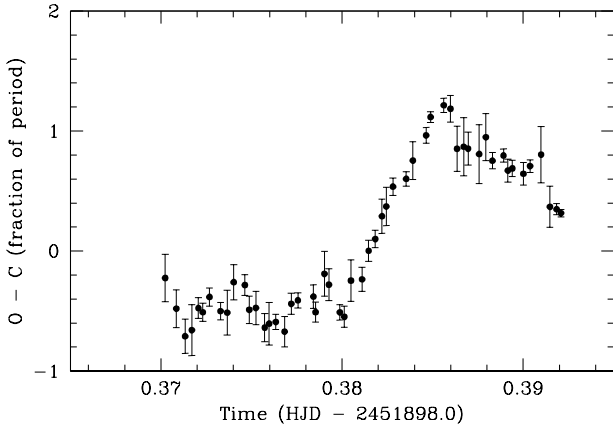


Figure 13. Phase variation in a section of run S6138.

computed for the test period 26.70 s. Here we see the reverse behaviour of what happens in Run S7222: the sudden change from 26.70 s to 29.58 s, seen as the abrupt change in slope at 0.380 d, would imply a change from direct DNO to synodic DNO from a traveling wave with a period of 274 s. There is a QPO in the range 0.349 – 0.363 d with a period of 285 ± 3 s, which is not visible to us during the 0.370 – 0.400 d time frame.

3.4 QPO Harmonics

In Paper II we suggested that the QPO signal arises from a traveling wave in the inner disc, obscuring and/or reflecting light from the central source. This is supported by the appearance of synodic DNOs, explained as reprocessing by the traveling wave. The existence of first and second harmonics to the QPOs does not have a geometrical explanation of the sort we invoke for the DNO harmonics; it appears more likely that the excitation mechanism for the traveling wave

changes as the inner edge of the disc recedes to regions of weaker field strengths.

This in turn could suggest an alternative model for the behaviour of the DNOs. If the excitation mechanism of the traveling wave manages to excite the first or second harmonic of the wave it will produce a double or triple humped QPO profile. The rotating DNO beam will then generate harmonic synodic DNOs at twice or three times the fundamental synodic DNO frequency. The appearance of the 1st and 2nd harmonic DNOs at about the same times as the corresponding QPO harmonics is in harmony with this model.

This model has the advantage of automatically preserving the $P_{QPO}/P_{DNO} \sim 15$ relationship, but less in its favour is that we sometimes see 1st and 2nd harmonic DNOs simultaneously, which requires similar excitation of both harmonics of the traveling wave. The rapid apparent jumps from direct to synodic DNOs, seen in the previous Section, are also not a simple consequence of this model. But the existence of the QPO harmonics does allow, perhaps even demand, some contribution to the DNO harmonics, and we add this to the *mélange* already outlined above.

3.5 Discussion

As pointed out in Paper III, the measured $v \sin i$ for the white dwarf in VW Hyi, which in combination with a mass and therefore radius of the white dwarf primary provides a rotation period, suggests that the lpDNOs are caused by two-pole accretion onto the surface of the primary, i.e. the rotation period of the primary is ~ 170 s. We hypothesized that variations of P_{lpDNO} can occur because of feeding gas onto different magnetic field lines that connect to the surface of the differentially rotating primary. Our conclusion here that the ordinary DNOs seen in the late phases of outburst involve two accretion zones, and that the angular velocity of the region containing those zones is slowed to approximately the same value as that of the underlying white dwarf is in accord with this interpretation of the lpDNOs.

At first sight it might be thought that there is incompatibility between our interpretation of the increase of P_{DNO} in the final stage of outburst, as a rapid deceleration of the equatorial belt, and the HST observations of a belt that is still rotating near Keplerian velocity days or weeks after outburst (Section 1). However, in the LIMA model the magnetic field (other than the weak field of the primary) is generated by shearing in the accretion flow onto and within the belt, so there is a selection effect at work – the accretion spots that create the DNOs are regions of maximum field strength, which are not necessarily regions of high angular velocity but rather are in regions of highest shear. In the generation of the field and the efficiency of magnetically channeled accretion there is a positive feedback mechanism – accretion torque increases shear which in turn enhances the field and ensures continual and increasing capture of accreting gas.

The phase of strong deceleration in VW Hyi implies strong shear and it is therefore not surprising that DNOs of greatest amplitude appear at that time. The disappearance of DNOs at $T \sim 1.4$ d may therefore be the result of most of the belt having become nearly uniform in angular velocity, near that of the underlying star, leaving only a narrow belt

of rapid rotation and a relatively small shear zone that loses angular momentum much more slowly (through friction with the stellar surface and through now weak magnetic coupling to the disc). This could also be the prime reason why magnetically controlled accretion, with its DNOs signature, is rare in quiescent dwarf novae.

VW Hyi remains unique as the only dwarf nova showing DNOs throughout the whole of its outburst. It would be useful to find another dwarf nova for which similar phenomena can be studied and compared with VW Hyi. Gänsicke, Beuermann & Thomas (1997) have pointed out that many of the general properties of EK TrA strongly resemble those of VW Hyi, though the latter has an \dot{M} about five times larger. EK TrA is not listed in the CVs that are known to have DNOs (Warner 2004). Recognizing that it would be of great value to have a second dwarf nova that shows DNOs right down to the beginning of quiescence we observed EK TrA at the end of its May 2004 outburst, at $m_V \sim 14.9$, but no DNOs were present.

4 QPOS IN X-RAY BINARIES

Much of the phenomenology of rapid oscillations in CVs described above resembles the behaviour of QPOs in X-Ray binaries (XRBs), so we will give a brief overview of the latter. Two distinct frequency domains exist among those XRBs that possess QPOs (which are often only intermittent): high frequency QPOs that are at \sim hundreds of Hz and low frequency QPOs that are at \sim tens of Hz. The hfQPOs usually are double, with the separation varying far less than the frequencies themselves (as \dot{M} changes). These appear to be the equivalent of double DNOs in CVs, but the frequency separation is close to the rotation frequency of the compact object, rather than to a more slowly moving traveling wave as in the CVs.

During X-Ray bursts on neutron star XRBs a third QPO frequency domain can appear, lying midway between the hfQPOs and lfQPOs. This contains oscillations variable in frequency that have been attributed to expanding gas (heated by thermonuclear runaway) on the surface of the neutron star, which slips relative to the surface and therefore does not represent precisely the rotation period of the star (van der Klis 2000, 2005). These are similar in behaviour to the lpDNOs that we see in CVs.

In XRBs, both for neutron star and black hole systems, the hfQPOs are at ~ 15 times the frequency of the lfQPOs (Belloni et al. 2002) and maintain this value as variations in \dot{M} change the frequencies in the neutron star binaries (in black hole binaries[§] the frequencies are almost invariant in each system (McClintock & Remillard 2005) but this may be due to the activity taking place in the vicinity of the innermost stable circular orbit (van der Klis 2005)). Identifying hfQPOs as the equivalent to DNOs in CVs, and lfQPOs as equivalent to the CV QPOs, we see the similarity in behaviour of XRBs and CVs, including the response to changing \dot{M} in VW Hyi, as was first pointed in Paper II and generalized in Paper III.

[§] Note that most of the discrepant points in the correlation for black hole binaries have been removed – see Kluźniak et al. (2005).

A further aspect of hfQPOs in XRBs is that some systems show harmonic structures (Remillard et al. 2002). Specific examples are XTE J1550-564 which has strong modulations near 276 and 184 Hz and some power at 92 Hz, which are in the ratios 3:2:1, GRO J1655-40 which has 450 and 300 Hz oscillations (Strohmayer 2001), and H 1743-322 which has 240 and 160 Hz QPOs (Homan et al. 2005). Other examples for black hole XRBs are given by McClintock and Remillard (2005). Abramowicz et al. (2003) make a case for ratio 2:3 frequencies in the neutron star XRB Sco X-1.

There have been a number of attempts to understand the XRB QPOs (see reviews by van der Klis (2000, 2005) and Psaltis (2002)), but more recently the extension of the Psaltis-Belloni-van der Klis (1999) relationship (that $P_{QPO} = 15 \times P_{DNO}$) to CVs (Paper II; Mauche 2002) has shown that theories requiring strong gravity may not be necessary. Among them are those that enable both neutron and black hole XRBs to accrete into a rotating magnetosphere, as in the LIMA model for CVs. One example is the Robertson-Leiter model that allows proto-black holes to delay collapse towards their event horizons and so maintain a magnetic moment almost indefinitely (Robertson & Leiter 2002, 2003). Another is the Titarchuk and Wood (2002) model that associates the high frequency (DNO) oscillations with the Keplerian frequency at the inner edge of the disc and the low frequency ones (QPOs) with magnetoacoustic oscillations that are excited by the transition to sub-Keplerian flow at the inner edge. Of these, the former more closely resembles the model that we have proposed for CVs.

A word of caution is necessary. There are several frequencies observed in neutron star binaries and it is only the highest of these that correlates closely with the low frequency. There are, however, strong correlations among the other frequencies. In black hole binaries the highest frequency analogue is not observed, but there is a correlation between other frequencies similar to that in neutron star binaries. It is this that provides the black hole / neutron star / white dwarf general correlation (van der Klis 2005).

Our new observations, exhibiting for the first time 3:2:1 relationships among CV DNOs, are a possible indication that strong gravity may not be essential for modeling DNOs and QPOs in compact binaries. It may also be the case that different physical processes are involved (e.g., Kluźniak et al. 2005).

5 CONCLUSIONS

VW Hyi continues to provide unprecedented behaviour in its rapid variations. No other dwarf nova is yet known that shows such a range of phenomena; whether this is connected with the sustained and increasing prominence of oscillations late in outburst is not known – no other dwarf nova has shown this either. The rapid increase in period of the DNOs, at a rate greater than that observed in other declining dwarf novae, which we have attributed to a phase of propelling and deceleration of an equatorial accretion belt, has been shown here to be accompanied by the appearance of first and second harmonics in both DNOs and QPOs. These are again unique to VW Hyi as a dwarf nova, but bear similarities to harmonics seen in the QPOs of X-Ray binaries.

Whereas most of the behaviour of the DNOs can be understood in terms of accretion from a disc onto a freely rotating equatorial accretion belt, that of the QPOs has not been fully explained.

Tests of the models suggested in this series of papers could be made from measuring the amplitude and phase changes of DNOs and QPOs observed in eclipsing CVs, and from detection of polarization modulated at the periods of the DNOs. These will require large telescopes to provide the necessary good signal/noise.

ACKNOWLEDGMENTS

We are indebted to the late Danie Overbeek and to Rod Stubbings and Albert Jones for alerting us to outbursts of VW Hyi. We also thank Rod Stubbings for providing us with his long term light curve of VW Hyi. Retha Pretorius kindly contributed the run S7301 light curve. BW's research is supported by the University of Cape Town; PAW is supported by research funding from the National Research Foundation and the University of Cape Town, and by a strategic grant to BW from the University of Cape Town.

REFERENCES

- Abramowicz M.A., Bulik T., Bursa M., Kluźniak W., 2003, *A&A*, 404, 21L
- Alpar M.A., Shaham J., 1985, *Nature*, 316, 239
- Belloni T., Psaltis D., van der Klis M., 2002, *ApJ*, 572, 392
- Gänsicke B.T., Beuermann K., 1996, *A&A*, 309, 47L
- Gänsicke B.T., Beuermann K., Thomas H.-C., 1997, *MNRAS*, 289, 388
- Godon P., Sion E.M., Cheng F.H., Szkody P., Long K.S., Froning C.S., 2004, *ApJ*, 612, 429
- Haefner R., Schoembs R., Vogt N., 1979, *A&A*, 77, 7
- Hellier C., Mukai K., Beardmore A.P., 1997, *MNRAS*, 292, 397
- Hellier C., Mason K.O., Rosen S.R., Cordova F.A., 1987, *MNRAS*, 228, 463
- Homan J., Miller J.M., Wijnands R., van der Klis M., Belloni T., Steeghs D., Lewin W.H.G., 2005, *ApJ*, 623, 383
- Kluźniak W., Lasota J.-P., Abramowicz M.A., Warner B., 2005, *A&A*, 440, 25L
- Lamb D.Q., 1988, in Coyne G.V., et al., eds., *Polarized Radiation of Circumstellar Origin*, Vatican Observatory, Vatican, p. 151
- Lamb F.K., Shibazaki N., Alpar M.A., Shaham J., 1985, *Nature*, 317, 681
- Mauche C.W., 2002, *ApJ*, 580, 423
- McClintock J.E., Remillard R.A., 2005, in Lewin W.H.G., van der Klis M., eds., *Compact Stellar X-Ray Sources*, Cambridge Univ. Press, Cambridge, in press
- Nauenberg M., 1972, *ApJ*, 175, 417
- O'Donoghue D., 1995, *Baltic Astr.*, 4, 517
- Paczynski B., 1978, in Zytkow A., ed., *Nonstationary Evolution of Close Binaries*. Polish Scientific Publ., Warsaw, p. 89
- Peterson J.A., 1980, *ApJ*, 241, 247
- Pfeiffer H.P., Lai D., 2004, *ApJ*, 604, 766
- Pretorius M.L., 2004, MSc Thesis, University of Cape Town
- Psaltis D., 2002, *Adv.Sp.Res.*, 481, 281
- Psaltis D., Belloni T., van der Klis M., 1999, *ApJ*, 520, 262
- Rappaport S.A., Fregeau J.M., Spruit H., 2004, *ApJ*, 606, 436
- Remillard R.A., Muno M.P., McClintock J.E., Orosz J.A., 2002, *ApJ*, 580, 1030
- Robertson S.L., Leiter D.J., 2002, *ApJ*, 565, 447
- Robertson S.L., Leiter D.J., 2003, *ApJ*, 596, 203L
- Romanova M.M., Ustyugova G.V., Koldoba A.V., Lovelace R.V.E., 2004, *ApJ*, 610, 920
- Schechter P.L., Mateo M., Saha A., 1993, *PASP*, 105, 1342
- Sion E.M., Cheng F.H., Huang M., Hubeny I., Szkody P., 1996, *ApJ*, 471, L41
- Sion E.M., Cheng F.H., Godon P., Urban J.A., Szkody P., 2004a, *AJ*, 128, 1834
- Sion E.M., Cheng F.H., Gänsicke B.T., Szkody P., 2004b, *ApJ*, 614, 61L
- Sion E.M., Winter L., Urban J.A., Tovmassian G.H., Zharikov S., et al., 2004c, *AJ*, 128, 1795
- Smith K.W., Bonnell I.A., Lewis G.F., 1995, *MNRAS*, 276, 263
- Strohmayr T.E., 2001, *ApJ*, 552, 49L
- Titarchuk L., Wood K., 2002, *ApJ*, 577, 23L
- Uzdensky D.A., 2004, *Ap&SS*, 292, 573
- van der Klis M., 2000, *ARA&A*, 158 233
- van der Klis M., 2005, in Lewin W.H.G., van der Klis M., eds., *Compact Stellar X-Ray Sources*, Cambridge Univ. Press, Cambridge, in press
- Warner B., 1983, in Livio M., Shaviv G., eds., *Cataclysmic Variables and Related Objects*, Reidel, Dordrecht, p. 269
- Warner B., 1986, *MNRAS*, 219, 347
- Warner B., 1987, *Lect. Notes Phys.*, 274, 384
- Warner B., 1995a, *Cataclysmic Variable Stars*, Cambridge Univ. Press, Cambridge
- Warner B., 1995b, in Buckley D.A.H., Warner B., eds., *ASP Conf. Ser. Vol. 85, Cape Workshop on Magnetic Variables*. Astron. Soc. Pac., San Francisco, p. 343
- Warner B., *PASP*, 2004, *PASP*, 116, 115
- Warner B., Robinson E.L., 1972, *Nature Phys. Sci.*, 239, 2
- Warner B., Woudt P.A., 2002, *MNRAS*, 335, 84 (Paper II)
- Warner B., O'Donoghue D., Wargau W., 1989, *MNRAS*, 238, 73
- Warner B., Woudt P.A., Pretorius M.L., 2003, *MNRAS*, 344, 1193 (Paper III)
- Woudt P.A., Warner B., 2002, *MNRAS*, 333, 411 (Paper I)